Reflection from elastic wedges of different thickness profiles

A. Karlos [1], **S. Elliott** [1] **and J. Cheer** [1]
[1] Institute of Sound and Vibration Research, University of Southampton,
Southampton, SO17 1BJ, United Kingdom
e-mail: **A.Karlos@soton.ac.uk**

Abstract
An elastic wedge whose thickness varies with axial position according to a power law can act as an absorber of incident flexural waves and thus as an anechoic termination. Ideally, if the wedge is tapered down to zero thickness, the incident wave slows down to zero propagation velocity at the edge, thus never reaching the boundary, and, so, not undergoing reflection. In practice, however, a small truncation of the wedge always occurs, due to manufacturing restrictions, leading to non-zero thickness at the edge, so that some reflection does occur. In this paper, alternative thickness profiles are examined, such as the power-cosine, the exponential and the Gaussian profile, the latter two inevitably having a truncation within a finite length. A method based on the WKB approximation is used in order to calculate the reflection coefficient of a structure comprising a wedge connected to a uniform plate. Higher-order WKB approximations are also applied. Results are compared with those from a Finite Element analysis.

1 Introduction

In various engineering applications, vibration damping is of great importance. A novel idea for attenuating structural vibrations was proposed by Mironov in [1]. In that article, it was theoretically predicted that a wedge-like plate which tapers according to a quadratic law down to zero thickness, undergoing one-dimensional bending, will cause incident waves to slow down to zero propagating velocity at the vicinity of the vanishing free edge; therefore, the waves will not reach the boundary and they will not be reflected. The energy carried by the waves will be dissipated by the arbitrarily weak damping of the material of the structure at the region near the free edge. This phenomenon has come to be known as the 'acoustic black hole' effect. It can be shown with the same type of analysis as the one carried out in [1] that this theoretical result holds for any non-uniform plate with a power-law thickness profile of order greater than or equal to two, that is, with thickness varying as $h_p = h_0 (1 - x/x_0)^n$, where h_0 is the thickness at the input end of the wedge and x_0 is the length of the wedge, the point $x = x_0$ corresponding to the edge of vanishing thickness, as depicted in Figure 1. The same qualitative conclusions hold for a beam of constant width, since the equation of motion of such a system is similar to that describing one-dimensional bending waves in a plate.

It was also demonstrated in [1] that even a small truncation at the edge of the plate, which inevitably occurs in practice due to manufacturing restrictions, introduces considerable reflection. In order to overcome this problem, Krylov and Tilman proposed applying thin layers of viscoelastic material on the sides of the wedge [2]. It was theoretically predicted in that article that the use of such damping layers greatly reduces the reflection from the truncated wedge, thus enhancing the damping effect due to the tapering geometry. This idea has been further elaborated on, both in terms of mathematical modelling and experimentally in a number of articles, as has been reviewed in [3].

The wedges examined in [1] and [2] are considered to be driven internally, that is, an incident flexural wave originating inside the wedge is travelling towards the free edge. Therefore, this approach only accounts

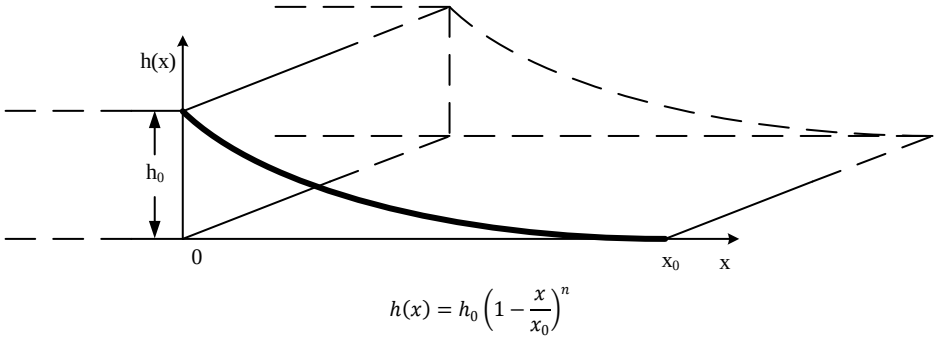

Figure 1: Elastic wedge of power-law thickness profile, ideally tapered down to zero thickness, terminating a uniform plate.

for reflection due to the edge. In practice, however, a wedge usually forms the termination of a uniform waveguide, so that there is an additional source of reflection due to the junction of the uniform and non-uniform parts of the system. Such composite systems have been examined in the literature using different mathematical modelling approaches. In [4], a rectangular uniform plate with one of its edges terminated as a power-law wedge is examined, using a matrix formulation for the various boundary conditions, including the continuity and equilibrium conditions at the junction of the uniform plate with the wedge. The vertical displacement in the wedge is represented by an approximate analytical solution of the two-dimensional equation of motion, so that oblique incidence is also accounted for. The analysis focuses on driving-point and transfer mobility. A numerical solution of the one-dimensional flexural wave equation is implemented in [5], where the impedance matrix method is employed for the formulation of the matrix equation to be solved numerically, thus yielding the reflection coefficient for a wave travelling towards the wedge from the uniform part. Yet another methodology was presented more recently in [6], where a wavelet expansion is used for the vertical displacement of the wedge, giving good correspondence with measurements. In all three of these articles, mathematical models for thin damping layers are included.

As regards mathematical models which are based on an analytical representation of the displacement field in the wedge, it is the first-order WKB approximation that is usually implicitly used in the literature. Such is the case in [1], as well as in [2], where it is referred to as the geometrical acoustics approximation, and in [4]. In the case where the reflection only due to the free end is considered, as in [1] and [2], the accuracy of the approximation is not easily assessed by comparison with experimental results. However, theoretically predicted results have been compared with experimental ones for example in [4], where the mathematical model includes the effect of the junction to the flexural wave. Even though the authors recognise qualitatively similar trends and some quantitative correspondence of the predicted and measured resonance frequencies in parts of the spectrum in that study, the use of different boundary conditions for the mathematical model and the experiment do not allow for a valid comparison between the two.

The validity of the WKB method is linked to a set of conditions that need to be satisfied so that the solution is an asymptotic solution to the differential equation under study [7]. Furthermore, an additional condition has to be satisfied, which is different for different orders of approximation, so that the truncation of the infinite-order solution up to a term of finite order form a valid approximation. In the literature of non-uniform flexural waveguides, for example in [1] and [2], only one of the validity conditions is typically used, which can be expressed as the requirement that the relative change of the wavenumber within the length of the order of a wavelength be negligible, usually expressed mathematically as

$$\left|\frac{k'}{k^2}\right| \ll 1, \tag{1}$$

where $k(x, \omega)$ is the space- and frequency-dependent wavenumber function within the waveguide and the prime denotes differentiation with respect to the spatial coordinate x. In [8] and [9], the quantity in the left side of condition (1) is used as a means of assessing the performance of a wedge in terms of reflection in correlation with the reflection coefficient predicted with a Finite Element model.

In the present article, an analytical method is used to calculate the reflection coefficient from a wedge driven from a semi-infinite uniform plate. It is shown that the usually employed first-order WKB approximation may give results that are significantly divergent from those obtained with a Finite Element model. Moreover, it is demonstrated that higher-order approximations may greatly improve the analytical prediction of the reflection coefficient.

Alternative profiles for the thickness variation may also be used, which still manifest the effect of suppressed reflection due to the decrease of propagation velocity towards the tapering edge of the non-uniform plate. An exponential profile with thickness varying as $h_e = h_0 e^{-\beta x}$, with $\beta > 0$, is considered, which forms the limit of a power-law profile with fixed length and maximum and minimum thickness as the order of the power tends to infinity, that is, $\lim_{n\to\infty} h_p(n) = h_e$, where $h_p = h_0 \left(1 - x/x_0\right)^n$ is the power-law profile of order n. An exponential wedge of finite length inevitably has a truncated edge, which does not pose a restriction to real applications, since the ideal taper of zero edge thickness is practically unrealisable. It can also be shown that the modulus of the inner reflection coefficient of the exponential wedge is smaller than any finite-length power-law wedge of the same dimensions, that is, the exponential produces less reflection due to truncation. Therefore, the exponential profile may be considered optimal in terms of inner reflection within the family of power-law thickness profiles. A practical disadvantage of the exponential wedge is that it becomes much thinner than a power-law profile before the edge, so that it is much acuter and thus harder to manufacture and more prone to damage.

In a wedge connected to a uniform plate, apart from the truncated edge, the junction of the two parts also introduces reflection, due to discontinuity of slope. Therefore, there is motivation to search for thickness profiles whose slope starts from zero, so that they may be smoothly connected to a constant profile. It was presented in [2] that a wedge with a sinusoidal thickness profile raised to a power equal to or greater than two also leads to propagation velocity which tends to zero towards the edge, if the wedge is ideally tapered down to zero thickness. In the present article, a sinusoidal profile in the form of a power-cosine is examined, that is, with its thickness varying as $h_{pc} = h_0 \cos^n\left(\pi x/(2x_0)\right)$, where x_0 is the length where the thickness becomes zero. Similarly to the power-law and exponential profiles, the Gaussian profile with thickness variation $h_g = h_0 e^{-\gamma x^2}$, with $\gamma > 0$, appears to form the limit of the power-cosine profile as the order of the power tends to infinity, that is, $\lim_{n\to\infty} h_{pc}(n) = h_g$, thus producing an inner reflection coefficient which is smaller than that of any power-cosine wedge throughout the spectrum. The power-cosine profiles have the advantage of not having a discontinuity of slope at the junction with a uniform plate, while producing a vanishing propagation velocity at their free edge in the ideally tapered case. The special characteristics of the various profiles are presented by means of the reflection coefficient calculated with Finite Element models as well as with WKB approximations of order up to three.

2 Methods

The system to be considered in this study is a truncated wedge-like non-uniform plate connected to a semi-infinite uniform plate. Incident waves are travelling on the x-direction from the uniform part towards the wedge, as depicted in Figure 2. The equation describing the one-dimensional flexural harmonic vibration of a thin plate with varying thickness, $h(x)$, is

$$\left[D(x)w''(x)\right]'' - \omega^2 \rho h(x) w(x) = 0, \tag{2}$$

where $w(x)$ is the vertical displacement amplitude of the midplane of the plate, ω is the angular frequency, ρ is the density of the material of the plate, $D(x) = \rho c_p^2 h^3(x)/12 = E h^3(x)/\left(12(1-\sigma^2)\right)$ is the bending stiffness, E is Young's modulus, σ is Poisson's ratio, and c_p is the velocity of quasi-longitudinal waves

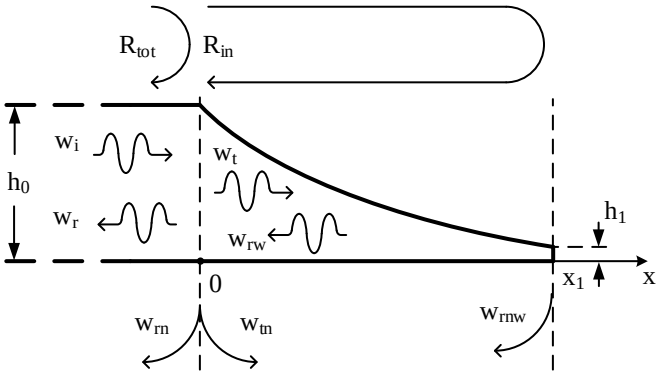

Figure 2: Truncated elastic wedge connected to a uniform plate. The various travelling and evanescent waves are shown, as well as the inner and total reflection coefficients.

in a thin plate, given by $c_p = \left[E/\left(\rho\left(1-\sigma^2\right)\right)\right]^{1/2}$ [10]. The prime denotes differentiation with respect to the spatial variable x. The harmonic time dependence of the displacement is assumed to be $e^{i\omega t}$. It should be mentioned that the displacement is also dependent on frequency. However, since the equation of motion involves differentiation only with respect to the spatial variable, the dependence on frequency may be omitted for notational convenience. In consequent analysis, the spatial dependence is also often omitted for simplicity; it should be remembered that the displacement and its derivatives, as well as the bending stiffness and the thickness, are spatially varying in the non-uniform part of the waveguide.

2.1 The WKB approximation

Equation (2) is not analytically solvable for an arbitrary variation of the thickness. Therefore, it either has to be solved by some numerical method or an analytical approximation may be used. The WKB is a method for analytical approximations of arbitrarily high order for differential equations; a systematic presentation of the method can be found, for example, in [7]. Usually in vibration literature, the first-order approximation is used, and it is commonly referred to simply as the WKB approximation. The first-order WKB approximation for beams and plates was derived by Pierce in [11], based on considerations of energy conservation. A more systematic approach, similar to the one in [7], is presented in [12], which readily allows for the use of higher-order approximations.

For the general formulation of the WKB approximation, a perturbation factor has to be included in the differential equation. In the case of Equation (2), a perturbation factor given by $\epsilon = \omega^{-1/2}$ may be included, so that the equation takes the form

$$\epsilon^4 \left[Dw''\right]'' - \rho h w = 0. \tag{3}$$

A trial solution for the vertical displacement is used, having the form

$$w = e^{\epsilon^{-1} \sum_{n=0}^{\infty} S_n \epsilon^n}, \epsilon \to 0, \tag{4}$$

where the functions S_n are spatially and spectrally variable. In strict mathematical notation, the sign of equality in relation (4) should be substituted by $\sim$, to express the fact that this relation is an asymptotic solution to the differential equation, as the perturbation factor tends to zero, and not an exact solution; a looser notational convention is followed in this analysis, following the engineering literature. The fact that when the perturbation factor tends to zero the frequency tends to infinity and vice versa implies that the WKB

solution (4) constitutes a better approximation at high frequencies and ceases to be a good approximation at low frequencies. As pointed out in [13], however, Equation (2) only applies below the frequencies where the rotational inertia is significant and so the WKB solution to Equation (2) only strictly applies over a given bandwidth.

Substitution of relation (4) into Equation (3) yields a polynomial equation for ϵ. For the polynomial equation to hold for any ϵ, all coefficients of the powers of ϵ have to be equal to zero, so that an infinite set of differential equations is obtained, the first four of which are

$$S_0'^4 = \frac{\rho h}{D} = \frac{12}{c_p^2 h^2}, \tag{5}$$

$$S_1' = -\frac{3}{2}\frac{S_0''}{S_0'} - \frac{1}{2}\frac{D'}{D}, \tag{6}$$

$$S_2' = -\frac{3}{2}\frac{S_1'^2}{S_0'} - \frac{3}{2}\frac{S_1''}{S_0'} - 3\frac{S_0''S_1'}{S_0'^2} - \frac{S_0'''}{S_0'^2} - \frac{3}{4}\frac{S_0''^2}{S_0'^3} - \frac{3}{2}\frac{D'}{D}\frac{S_1'}{S_0'} - \frac{1}{4}\frac{D''}{D}\frac{1}{S_0'} - \frac{3}{2}\frac{D'}{D}\frac{S_0''}{S_0'^2} \tag{7}$$

and

$$\begin{aligned} S_3' = &-\frac{S_1'^3}{S_0'^2} - \frac{3}{2}\frac{D'}{D}\frac{S_1'^2}{S_0'^2} - 3\frac{S_1'S_2'}{S_0'} - \frac{3}{2}\frac{D'}{D}\frac{S_2'}{S_0'} - \frac{3}{2}\frac{S_2''}{S_0'} - \frac{S_1'''}{S_0'^2} - \frac{1}{4}\frac{S_0''''}{S_0'^3} - \frac{1}{2}\frac{D''}{D}\frac{S_1'}{S_0'^2} - 3\frac{S_1'S_1''}{S_0'^2} - \\ &\frac{3}{2}\frac{D'}{D}\frac{S_1''}{S_0'^2} - \frac{S_0'''S_1'}{S_0'^3} - \frac{1}{2}\frac{D'}{D}\frac{S_0'''}{S_0'^3} - \frac{3}{2}\frac{S_0''S_1''}{S_0'^3} - \frac{1}{4}\frac{D''}{D}\frac{S_0''}{S_0'^3} - 3\frac{S_0''S_2'}{S_0'^2} - \frac{3}{2}\frac{S_0''S_1'^2}{S_0'^3} - \frac{3}{2}\frac{D'}{D}\frac{S_0''S_1'}{S_0'^3}. \end{aligned} \tag{8}$$

The WKB approximation of order N includes the first $N+1$ terms in the exponent of the solution (4), thus including the first $N+1$ WKB functions, that is, from S_0 up to S_N. Therefore, the first $N+1$ equations of the WKB formulation have to be serially solved, starting from the zeroth order. Equation (5), which is also called the eikonal equation, has four roots, namely

$$S_0' = \{\pm 1, \pm i\}\frac{12^{1/4}}{c_p^{1/2}h^{1/2}}, \tag{9}$$

where the factors defining the four distinct solutions are included in curly brackets. Integration with respect to x gives

$$S_0 = \{\pm 1, \pm i\}\int_0^x \frac{12^{1/4}}{c_p^{1/2}h^{1/2}}d\tilde{x}. \tag{10}$$

The lower limit of integration has been chosen to be at the junction of the uniform and non-uniform parts, where the origin for the x coordinate is set to be. Equation (6), also called the transport equation, may then be solved, giving

$$S_1 = \frac{3}{4}\ln\left(\frac{h_0}{h}\right). \tag{11}$$

The form of Equation (6) is such that the distinctive constant coefficients of S_0 cancel out, so that S_1 is the same for all four different solutions of the eikonal equation.

The first-order WKB solution to Equation (3) is found by including only the first two terms in the exponent of relation (4). Therefore, by virtue of Equations (10) and (11), the first-order WKB solution can be written as

$$w_1 = A\left(\frac{h_0}{h}\right)^{3/4} e^{\{\pm 1, \pm i\}\int_0^x k(\tilde{x})d\tilde{x}}, \tag{12}$$

where

$$k = \frac{12^{1/4}\omega^{1/2}}{c_p^{1/2}h^{1/2}}\left(1 - i\frac{\eta}{4}\right) \tag{13}$$

is the wavenumber function in the non-uniform plate, A is an arbitrary complex constant and η is the damping factor. The inclusion of the damping factor has been achieved by using a complex Young's modulus in the form of $E(1+i\eta)$, which, through the quasi-longitudinal velocity c_p and after appropriate simplifications due to the assumed small value of η, gives the complex wavenumber of Equation (13). The expected deviation of the WKB approximation at low frequencies mentioned earlier may be linked to the violation of the validity condition, relation (1), at low frequencies, as can be seen by use of the wavenumber function of Equation (13).

The second- and third-order WKB approximations may, accordingly, be written as

$$w_2 = A\left(\frac{h_0}{h}\right)^{3/4} e^{\{\pm 1,\pm i\}\int_0^x k(\tilde{x})d\tilde{x}+\omega^{-1/2}S_{2,j}} \tag{14}$$

and

$$w_3 = A\left(\frac{h_0}{h}\right)^{3/4} e^{\{\pm 1,\pm i\}\int_0^x k(\tilde{x})d\tilde{x}+\omega^{-1/2}S_{2,j}+\omega^{-1}S_{3,j}}, \tag{15}$$

respectively, where the subscript $j = \pm 1, \pm i$ denotes the different S_2 and S_3 functions corresponding to the four different S_0 functions; the S_2 and S_3 functions are obtained by integrating Equations (7) and (8), respectively. It should be noted that Equations (7) and (8) are in general not integrable analytically, so that numerical integration has to be applied.

2.2 Matrix formulation for calculating the reflection coefficients

The reflective behaviour of a wedge driven from a uniform plate, such as the one depicted in Figure 2, may be assessed by use of the ratio of the reflected wave, travelling in the negative-x direction in the uniform plate, to the incident travelling wave, evaluated at the junction of the uniform and non-uniform parts, where $x = 0$. This ratio is henceforth called the total reflection coefficient and is given by $R_{tot} = w_r(0)/w_i(0)$, in accordance with the notation shown in Figure 2.

The various wave components inside the wedge may be expressed in the form of WKB approximations of a specified order. The appropriate coefficient for the wavenumber has to be chosen to match with the direction and the qualitative type of each component; coefficients $-i$ and $+i$ correspond to positive-x and negative-x travelling waves, respectively, while coefficients -1 and $+1$ correspond to positive-x and negative-x evanescent waves, respectively. The wave components in the uniform part may be expressed as exponential functions with constant amplitude and constant wavenumber,

$$w_u = Ae^{\{+1,\pm i\}k_u x}, \tag{16}$$

where k_u is the spatially constant wavenumber in the uniform part; the appropriate one from the factors written in the curly brackets again needs to be chosen for each component. It should be noted that no incident nearfield wave is present in the uniform plate, since it is considered to be semi-infinite, and, hence, the factor of -1 is not included.

The displacement field in the uniform plate and in the wedge may be expressed as the superposition of the corresponding wave components, all of which will in general have different constant amplitude coefficients. The amplitude coefficients represent ratios of wave components evaluated at the coordinate origin, so that they may be thought of as reflection and transmission coefficients. These unknown coefficients may be calculated by applying the various boundary conditions of the system, which are the continuity of displacement and its slope and the equilibrium of bending moment and shear force at the junction, as well as the vanishing of bending moment and shear force at the free edge boundary, where the bending moment is given by $M = Dw''$ and the shear force by $V = -M'$ [10]. This procedure involves calculating up to the third derivatives of the wave components, which get increasingly complicated with increasing order of differentiation, and even more with increasing order of WKB approximation. Numerical differentiation has been used

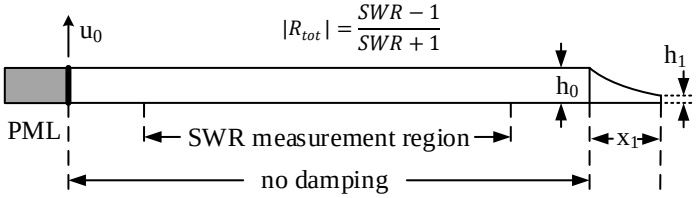

Figure 3: Schematic of a Finite Element model for a wedge connected to a semi-infinite uniform plate. A harmonic vertical velocity of constant amplitude u_0 is used as a source of excitation. A perfectly matched layer (PML) on the left end assures than no reflection occurs from that side. The standing wave ratio (SWR) is obtained by measuring the maximum and minimum displacement moduli over a region of the uniform plate away from sources of nearfield waves.

for the calculation of the second- and third-order derivatives of the second- and third-order WKB functions given in Equations (7) and (8). Solving the system of equations corresponding to the applied conditions yields, among others, the total reflection coefficient, R_{tot}, which is of primary interest, and the inner reflection coefficient, defined as $R_{in} = w_{rw}(0)/w_t(0)$, whose modulus is equivalent to the reflection coefficient used in [1] and [2].

A similar approach may be applied for a wedge ideally tapered down to zero thickness driven from a uniform plate. In this case, it is considered that all waves travelling or decaying towards the edge are completely attenuated, so that no reflected waves, either travelling or nearfield, are present in the wedge. Accordingly, no conditions need be applied at the vanishing edge, resulting in a four by four system of equations for the various reflection and transmission coefficients. In such a system, reflection occurs only at the junction, and the corresponding reflection coefficient, denoted by R_j in this analysis, expresses the reflective effect of the junction to incident waves.

2.3 Finite Element model

A Finite Element model was implemented in COMSOL Multiphysics 5.3 for calculating the modulus of the reflection coefficient of a wedge driven from a uniform plate. A qualitative illustration is given in Figure 3. The system is driven by applying a harmonic vertical velocity of constant amplitude to the uniform plate at a position away from the wedge. A perfectly matched layer is connected to the left end of the uniform plate in order to suppress reflections from this side, so that the model may simulate a semi-infinite system. Furthermore, the uniform plate is modelled as having no damping, so that travelling waves do not attenuate within it; damping is present only in the non-uniform part. The maximum and minimum displacement moduli are measured over a region of the uniform plate away from both the point of excitation and the junction with the wedge, in order to avoid measuring evanescent components. Therefore, the standing wave ratio is calculated from the relation $SWR = |w|_{max} \,/\, |w|_{min}$ [14]. Finally, the modulus of the total reflection coefficient is obtained from the following equation, [14],

$$|R_{tot}| = \frac{SWR - 1}{SWR + 1}. \tag{17}$$

It should be mentioned that, for accurate measurement of the maximum and minimum displacements, the region of measurement has to be long enough to include a wavelength of the lowest frequency examined. In the Finite Element simulations conducted here, 14456 two-dimensional solid elements were used for the uniform plate and 3939 to 8325 solid elements for the wedge, depending on the thickness profile.

3 Results and discussion

For the simulations of this study, wedges with properties as presented in Table 1 were used. The specific properties of the four different thickness profiles considered are summarised in Table 2, expressed with respect to given quantities. The quadratic profile constitutes the lowest-order power-law profile for which the propagation velocity vanishes at its ideal edge. A plot of the moduli of the inner and total reflection coefficients, along with the modulus of the junction reflection coefficient, which is present in an ideally tapered wedge of similar geometry, all calculated using the first-order WKB approximation, are shown in Figure 4. First of all, it can be seen that the total reflection coefficient fluctuates with frequency around the inner reflection coefficient. These fluctuations are the result of the frequency-varying interaction of an incident wave with the two sources of reflection, that is, the free edge and the junction. Secondly, the junction reflection coefficient retains high values at low frequencies, whereas it decreases down to very low values at higher frequencies. This may be linked to the fact that, at low frequencies, the discontinuity at the junction resembles a more abrupt thickness change, while at high frequencies, the flexural wavelength is smaller and can follow the change in thickness more easily, undergoing little reflection. Furthermore, the fluctuations of the total reflection coefficient around the inner reflection coefficient are greater in magnitude at lower frequencies, where reflection due to the junction is also strong. Moreover, the junction reflection coefficient in Figure 4 shows a peak at about 50 Hz, whereas it would be expected to decrease monotonically with increasing frequency. This result may be linked to the deteriorating validity of the WKB approximation as frequency decreases.

Geometrical properties	Value	Material properties	Value
Length of wedge (x_1)	0.3 m	Young's modulus (E)	$70 \cdot 10^9$ Pa
Thickness at junction (h_0)	0.01 m	Density (ρ)	2700 kg·m^{-3}
Thickness at edge (h_1)	10^{-4} m	Poisson's ratio (σ)	0.33
		Damping factor (η)	0.01

Table 1: Geometrical and material properties of the wedge model. Damping applies only to the non-uniform part of the waveguide.

Thickness profile type	Thickness variation	Length of ideal wedge	Decay parameter
Quadratic	$h_q = h_0 \left(1 - \frac{x}{x_0}\right)^2$	$x_0 = \frac{x_1}{1-\left(\frac{h_1}{h_0}\right)^{1/2}}$	-
Exponential	$h_e = h_0 e^{-\beta x}$	∞	$\beta = \frac{1}{x_1 \ln\left(\frac{h_0}{h_1}\right)}$
Power-cosine	$h_{pc} = h_0 \cos^n\left(\frac{\pi x}{2x_0}\right)$	$x_0 = \frac{\pi x_1}{2\arccos\left(\left(\frac{h_1}{h_0}\right)^{1/n}\right)}$	-
Gaussian	$h_g = h_0 e^{-\gamma x^2}$	∞	$\gamma = \frac{1}{x_1^2 \ln\left(\frac{h_0}{h_1}\right)}$

Table 2: Formulas for different thickness profiles.

A set of plots with results based on the WKB approximation for the different thickness profiles presented above is shown in Figure 5; the thickness variation of the different profiles is illustrated in Figure 5a. In the following results, a seventh-order cosine is used, due to the fact that its inner reflection coefficient practically coincides with that of a quadratic wedge, as can be seen in Figure 5d. It should be noted that this correspondence holds for the specific geometrical properties used; different properties will lead to different order for the inner reflection coefficient of a power-cosine wedge to match with that of the corresponding quadratic one. The matching of the inner reflection coefficients of the quadratic and the seventh-order cosine may be linked to the fact that their thickness profiles seem to be very similar towards the narrow edge of the wedge, as can be seen in Figure 5a, where the propagation velocity becomes small and most of the energy is dissipated.

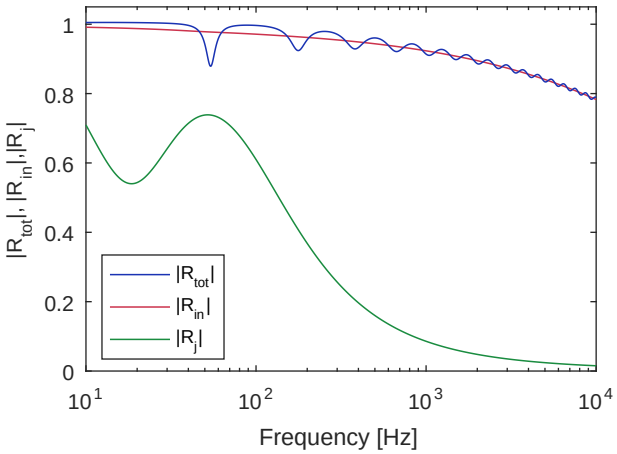

Figure 4: Moduli of the inner and total reflection coefficients of a truncated quadratic wedge, along with the modulus of the junction reflection coefficient of an ideally tapered quadratic wedge, using the first-order WKB approximation.

The phase velocity of a wave travelling in the wedge is given by $c_{ph} = \omega/\Re\{k\}$, where $\Re$ denotes the real part. The spatial variation of the phase velocity for the different profiles at 1000 Hz is shown in Figure 5c, where it can be seen that all profiles have a phase velocity of about 30 m·s^{-1} at the edge, where the thickness is 0.1 mm. The correspondence between thickness variation and phase velocity, through the wavenumber function of Equation (13), is apparent by comparison of Figures 5a and 5c.

The spectral variation of the modulus of the junction reflection coefficient for different profiles, calculated with the third-order WKB approximation, is plotted in Figure 5b. By inspection of the upper spectral region, it can be seen that the junction of the exponential wedge introduces more reflection than the junction of the quadratic wedge. This is expected, due to the fact that the exponential has greater absolute slope at the junction, thus introducing a more abrupt discontinuity. The power-cosine and Gaussian profiles, on the other hand, have junction reflection coefficients of modulus smaller than that of the quadratic at high frequencies, which may be related to the fact that the slope of these profiles at the junction is zero. At lower frequencies, however, it can be seen that the power-cosine and Gaussian profiles are predicted to produce greater reflection at the junction than the quadratic profile does, a result which contradicts the expected correspondence between slope and reflection at the junction. Nevertheless, this counter-intuitive result is verified by the Finite Element results, as can be seen in Figure 7, where the fluctuations of the power-cosine and Gaussian profiles are greater than those of the quadratic profile at low frequencies. This effect may be related to the presence of higher-order derivatives of the thickness variation in the solution.

Inconsistencies with the theory are present at low frequencies. The already mentioned violation of energy conservation, as well as fluctuations of the junction reflection coefficient, the latter occurring only for the exponential wedge at the currently used third-order of WKB approximation, are apparent. Such inconsistencies may again be linked to the issue of validity of the WKB at low frequencies.

Figure 5d shows the moduli of the inner reflection coefficients of the different thickness profiles. The inner reflection coefficient of the quadratic and the seventh-order cosine are practically indistinguishable, apart from the very low end of the spectrum, since the specific order of cosine was chosen with this criterion. Inspection of the corresponding thickness and phase velocity variations shown in Figures 5a and 5c, respectively, illustrates that the thinner part of the wedge is predominant in defining the inner reflection coefficient, since a slightly smaller thickness of the power-cosine in the thinner third of the wedge and, accordingly, a slightly smaller phase velocity, balance out the much greater thickness and phase velocity difference in the thicker two thirds. The inner reflection coefficient for the exponential wedge has an unexpected very narrow dip around 100 Hz; a plot of the same coefficient as calculated according to the analysis in [1] is also shown.

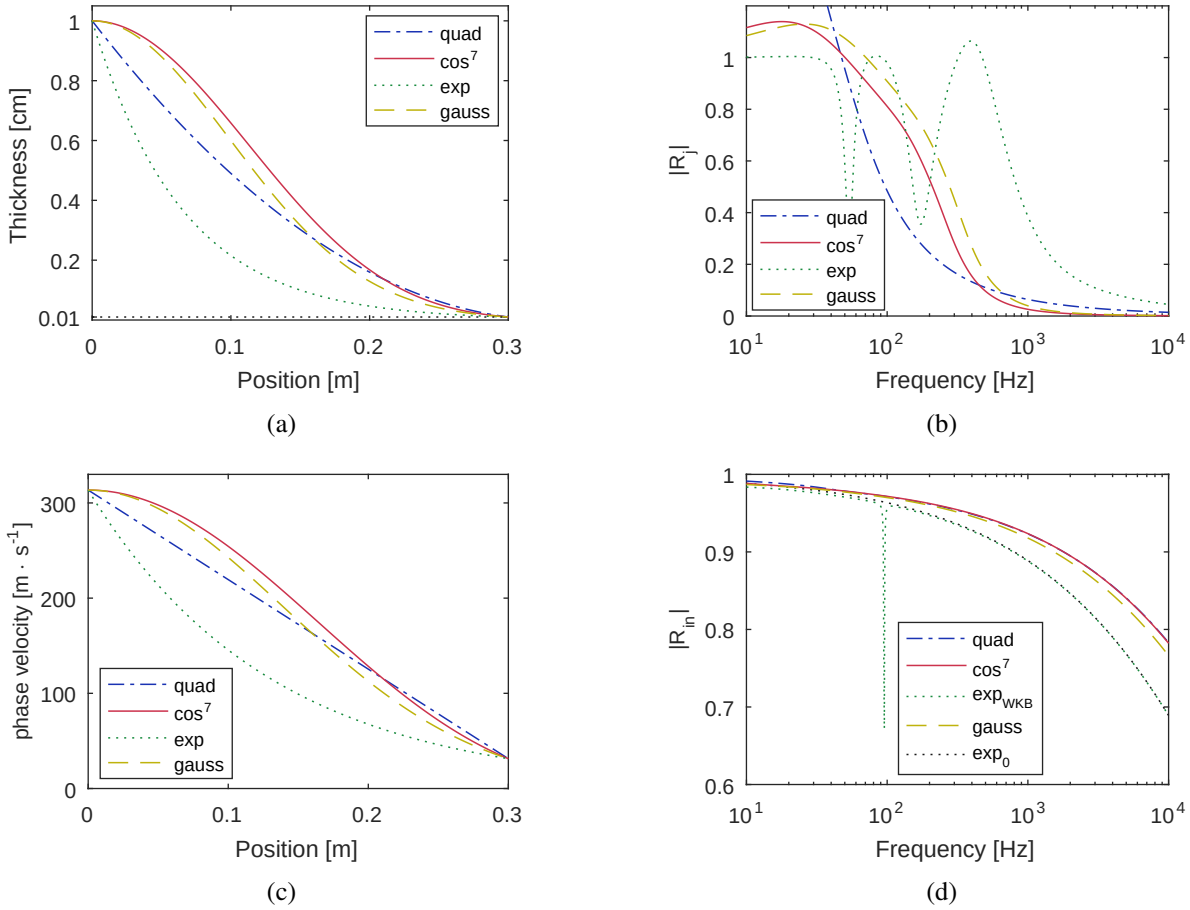

Figure 5: Properties of different profiles, namely a quadratic, a seventh-order cosine, an exponential and a Gaussian: (a) thickness variation, having a value of 0.1 mm at the thin edge, (b) spectral variation of the modulus of the junction reflection coefficient, calculated with the third-order WKB approximation, (c) spatial variation of the phase velocity at a frequnecy of 1000 Hz, (d) spectral variation of the modulus of the inner reflection coefficient, calculated with the first-order WKB approximation. The modulus of the inner reflection coefficient of the exponential wedge has an unexpected dip at around 100 Hz. A plot for the modulus of the inner reflection coefficient which is produced with the approach presented in [1], where the wedge is driven internally and evanescent waves are not taken into account, is therefore also shown for qualitative consistency with the rest of the results, labelled as exp_0.

It can be seen that the exponential clearly improves the inner reflection coefficient, as was mentioned earlier, which may also be illuminated by the fact that the phase velocity of the exponential acquires significantly smaller values than that of the quadratic. A similar conclusion was drawn in [2], where higher-order power-law wedges were found to produce less inner reflection. The Gaussian, on the other hand, presents a very small improvement compared to the quadratic and seventh-order cosine, which complies with the respective thickness and phase velocity variations.

A comparison of results for the modulus of the total reflection coefficient between the presented method based on the WKB approximation and Finite Element analysis for the different thickness profiles is shown in Figure 6. It may be generally observed that, for all the thickness profiles, the WKB results diverge from the Finite Element ones predominantly at lower frequencies, as is expected due to the deteriorating validity of the method. A second general observation is that the WKB results, especially from higher-order approximations, correspond well with those from Finite Elements as frequency increases, although a small deviation starts to be visible in the very upper end of the considered spectrum. Furthermore, the first-order WKB approximation does not give very good correspondence with Finite Element analysis for the total reflection coefficient, apart

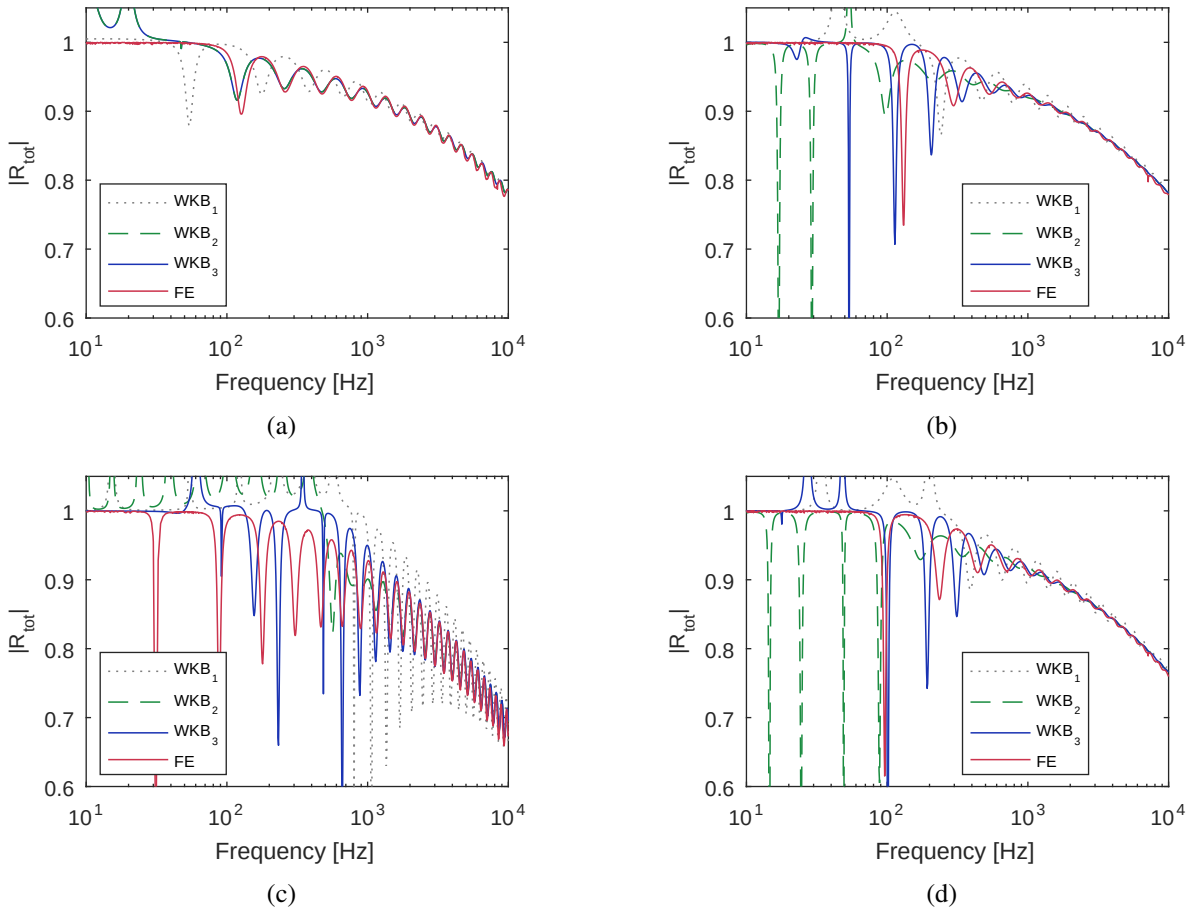

Figure 6: Comparison of the modulus of the total reflection coefficient calculated with the first three WKB approximations with corresponding results from Finite Element analysis, for different thickness profiles: (a) quadratic, (b) seventh-order cosine, (c) exponential and (d) Gaussian. For the quadratic, the third-order WKB solution is indistinguishable from the second-order one.

from frequencies at the upper end of the considered spectrum, failing in large part to predict similar resonance frequencies. On the other hand, the average level of the spectral fluctuations of the total reflection coefficient seems to be captured quite well, even by the first-order WKB approximation. This spectrally local average is linked to the inner reflection coefficient, as was mentioned earlier. Therefore, even though the inner reflection coefficient is not calculated by the current Finite Element model, the results for the total reflection coefficient imply that the former is well predicted even with first-order WKB considerations.

A central point of this analysis is the use of higher-order WKB approximations within the presented analytical model. A general overview of the results for all thickness profiles demonstrates the fact that higher-order approximations greatly improve the correspondence with the Finite Element model. In the case of the quadratic wedge, shown in Figure 6a, the second-order WKB already provides very good results in most of the spectrum, in this case above about 150 Hz, although correspondence is generally good even down to around 40 Hz. The third-order approximation does not produce any distinguishable improvement.

For the exponential wedge, shown in Figure 6c, inspection of the plots above about 400 Hz illustrates that the third-order WKB approximation provides significant improvement to the second-order one, which, in turn, greatly improves the first-order approximation. At lower frequencies, however, all WKB approximations up to third order fail to produce accurate results, also predicting values higher than one for the reflection coefficient. Furthermore, even for the higher-order approximations, the results are good above about 2 kHz. Interestingly, within the spectral region from about 900 Hz to roughly 1500 Hz, an oscillatory converging

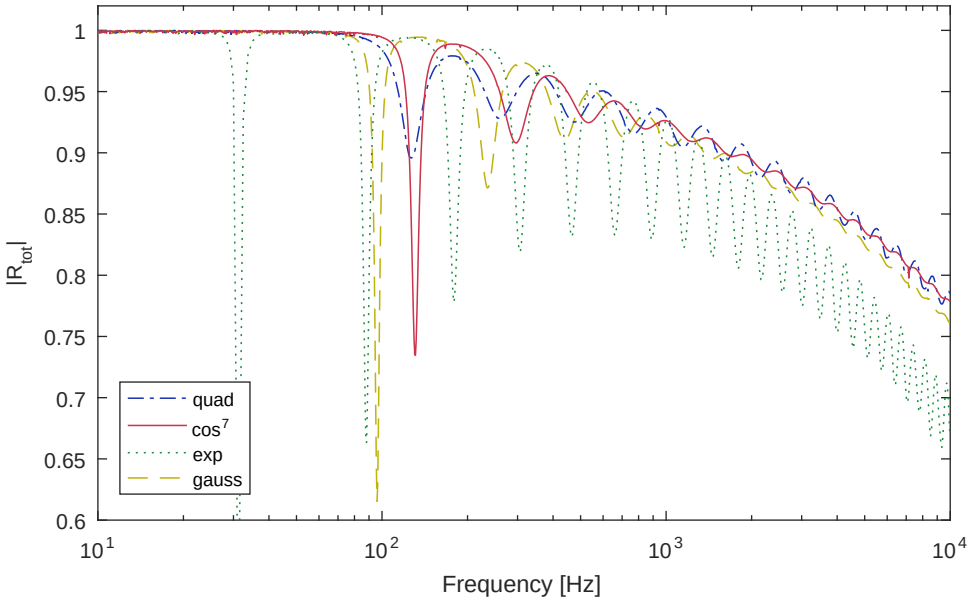

Figure 7: Modulus of the total refelction coefficient for different wedge thickness profiles, calculated from the Finite Element models.

trend for the solution seems to be followed, where consecutive orders of WKB approximation provide alternating overestimations and underestimations of the amplitude of spectral fluctuations of the total reflection coefficient. A similar behaviour is observed in Figures 6b and 6d for the power-cosine and Gaussian profiles, respectively. Finally, for the exponential as well as the power-cosine and Gaussian profiles, the third-order approximation seems to follow the Finite Element results starting from lower frequencies compared to the second-order approximation, thus providing better results in a greater part of the spectrum.

The seventh-order cosine and Gaussian wedges have similar reflection coefficients, as plotted in Figures 6b and 6d, respectively, which is expected due to the similarity of their thickness variation, as shown in Figure 5a. In the line of thought of the previous analysis for the quadratic and exponential wedges, the power-cosine and the Gaussian wedges seem to behave worse than the quadratic but much better than the exponential in terms of performance of the WKB method.

A comparative graph of the reflective behaviour of the different profiles is shown in Figure 7, where the moduli of the total reflection coefficients are plotted as calculated with Finite Element models. In the context of this comparative set-up, where all wedges are taken to have equal length and equal maximum and minimum thickness, the exponential wedge seems to provide considerably less reflection than the quadratic one over a large part of the spectrum. A power-cosine wedge with the same inner reflection coefficient as the quadratic comparatively reduces the fluctuation amplitude over most of the spectrum, above about 500 Hz in this case, though it increases it at low frequencies. The Gaussian wedge generally produces a small general decrease in the total reflection coefficient, again in compliance with the respective inner reflection coefficients shown in Figure 5d.

The reduction of the fluctuations that the power-cosine causes above some frequency, apart from being relatively small, does not improve the general level of reflection, since the order of the power of the cosine was chosen so as to give the same inner reflection as the quadratic. The Gaussian profile provides little improvement in that respect. Nevertheless, it should be noted that, in the considered context of comparison, the power-cosine and Gaussian wedges have considerably greater thickness than the quadratic along much of their length, as can be seen in Figure 5a. Apart from restrictions due to limitations in the realisability of very small thickness at the edge, which is taken to be the same for all wedges in this analysis, there are also

manufacturing restrictions on the acuteness of the wedge as represented by the length over which the wedge is very thin, a characterisation which is apparently of a qualitative nature. In light of this restriction, it can be commented that the exponential wedge is much acuter than the rest of the profiles. Therefore, longer Gaussian profiles may be manufactured, which would cause both less inner reflection, due to having a longer thin part in which the energy is dissipated, and less junction reflection, due to a longer thick part in which the slope varies more smoothly.

Two additional general comments need to be made. First, the reflection coefficients presented in this article generally have high values, due to the wedges being truncated, above 0.65 even at high frequencies. It is, however, well established in the literature, as reviewed in [3], that a combination of appropriate thickness variation and thin damping layers dramatically reduces reflection. Therefore, the current study focuses on one of the two main aspects of practically useful wedges. Second, all spectral results have been presented in a logarithmic scale for frequency, starting from a very low value of 10 Hz. The reason for this choice is that a key motivation for this study was to assess the behaviour of the WKB method in comparison with reference numerical results. Since it is known that the validity of results produced with the WKB method deteriorates with decreasing frequency, great resolution is required at low frequencies to facilitate comparison between the two methods. The fact that low frequencies cover a great part of the spectral plots might intuitively give a misleading impression that the less accurate results of the analytical method cover a wider spectrum than they actually do. In complement, it should be noted that the low end of the spectrum is less important in the study of wedges with absorbing properties, since, in general, their absorbing capability is poor at low frequencies.

4 Summary and Conclusions

A method has been presented for calculating reflection coefficients for a system consisting of a wedge connected to a semi-infinite uniform plate, which is based on the WKB approximation for the solution of the fourth-order equation of flexural vibrations of a thin plate. Four different thickness variation profiles for the wedge are considered, and the calculations are compared with those predicted from Finite Element models. The inner and junction reflection coefficients, obtained with the WKB-based method, are indirectly assessed through the above comparison of total reflection coefficients.

For all thickness profiles, the total reflection coefficient is found to fluctuate around the inner reflection coefficient along the spectrum. The amplitude of these fluctuations is related to the modulus of the junction reflection coefficient, so that, at low frequencies, where the junction reflection coefficient has high values, the fluctuations are great, whereas at higher frequencies, where the modulus of the junction reflection coefficient decreases, the amplitude of fluctuations also decreases.

The exponential profile produces less inner reflection due to the truncation but more reflection due to the junction than a quadratic wedge. Accordingly, the total reflection coefficient of the exponential fluctuates around a lower general level but with greater amplitude of fluctuations. In general, the effect of reduced inner reflection is found to be dominant, giving locally less total reflection in most of the spectrum compared to the quadratic. Furthermore, the power-cosine wedge, and, accordingly, its limit as the power tends to infinity, that is, the Gaussian, have the advantage of having zero slope at their thick end, so that they may be smoothly connected to a uniform plate. Such wedges are expected to produce less reflection at the junction compared to a power-law wedge. This appears to hold above some frequency; at low frequencies, however, the power-cosine wedge actually produces greater reflection at the junction than the quadratic.

The first-order WKB approximation is found to predict well the average level of reflection, represented by the inner reflection coefficient. However, it fails to predict the details of the fluctuations of the total reflection coefficient. Higher-order approximations are found to greatly improve the performance of the model, producing results that match the corresponding ones from Finite Element analysis very well above some frequency. The width of the spectrum over which correspondence with results from Finite Elements is good increases in accordance with the order of approximation, although this differs for the various profiles.

Acknowledgements

The authors would like to thank Kristian Hook for providing valuable help in the initial development of the Finite Element model, especially for the calculation of the SWR.

References

[1] M. A. Mironov, *Propagation of a flexural wave in a plate whose thickness decreases smoothly to zero in a finite interval*, Sov. Phys. Acoust., Vol. 34, No. 3 (1988), pp. 318-319.

[2] V. V. Krylov, F. J. B. S. Tilman, *Acoustic 'black holes' for flexural waves as effective vibration dampers*, Journal of Sound and Vibration, Vol. 274 (2004), pp. 605-619.

[3] V. V. Krylov, *Acoustic Black Holes: Recent Developments in the Theory and Applications*, IEEE Transactions on Ultrasonics, Ferroelectronics, and Frequency Control, Vol. 61, No 8 (2014), pp. 1296-1306.

[4] D. J. O'Boy, V. V. Krylov, V. Kralovic, *Damping of flexural vibrations in rectangular plates using the acoustic black hole effect*, Journal of Sound and Vibration, Vol. 329 (2010), pp. 4672-4688.

[5] V. B. Georgiev, J. Cuenca, F. Gautier, L. Simon, V. V. Krylov, *Damping of structural vibrations in beams and elliptical plates using the acoustic black hole effect*, Journal of Sound and Vibration, Vol. 330 (2011), pp. 2497-2508.

[6] Liling Tang, Li Cheng, Hongli Ji, Jinhao Qiu, *Characterization of acoustic black hole effect using a one-dimensional fully-coupled and wavelet-decomposed semi-analytical model*, Journal of Sound and Vibration, Vol. 374 (2016), pp. 172-184.

[7] Carl M. Bender and Steven A. Orszag, *Advanced Mathematical Methods for Scientists and Engineers*, McGraw-Hill, New York (1978).

[8] Philip A. Feurtado, Stephen C. Conlon and Fabio Semperlotti, *A normalized wave number variation parameter for acoustic black hole design*, J. Acoust. Soc. Am., Vol. 136, No 2 (2014), pp. 148-152.

[9] Philip A. Feurtado and Stephen C. Conlon, *Investigation of boundary-taper reflection for acoustic black hole design*, Noise Control Engineering Journal, Vol. 63, No 5 (2015), pp. 460-466.

[10] L. Cremer, M. Heckl and B. A. T. Petersson, *Structure-Borne Sound: Structural Vibrations and Sound Radiation at Audio Frequencies*, Springer-Verlag, Germany (2005).

[11] Allen D. Pierce, *Physical Interpretation of the WKB or Eikonal Approximation for Waves and Vibrations in Inhomogeneous Beams and Plates*, The Journal of the Acoustical Society of America, Vol. 48, No 1, Part 2 (1970), pp. 275-284.

[12] R. D. Firouz-Abadi, H. Haddadpour, A. B. Novinzadeh, *An asymptotic solution to transverse free vibrations of variable-section beams*, Journal of Sound and Vibration, Vol. 304 (2007), pp. 530-540.

[13] R. Nielsen, S. Sorokin, *The WKB approximation for analysis of wave propagation in curved rods of slowly varying diameter*, Proc. R. Soc. A, vol. 470 (2014)

[14] Lawrence E. Kinsler, Austin R. Frey, Alan R. Coppens and James V. Sanders, *Fundamentals of Acoustics, 4th Edition*, Wiley-VCH, United States of America (1999).